



HAL
open science

A contrasting seasonality of wind erosivity and wind erosion between Central and Western Sahel

C. Pierre, J.L. Rajot, I. Faye, G.S. Dorego, C. Bouet, B. Marticorena, G. Bergametti, A. Ka, B. Amar, A. Tall, et al.

► **To cite this version:**

C. Pierre, J.L. Rajot, I. Faye, G.S. Dorego, C. Bouet, et al.. A contrasting seasonality of wind erosivity and wind erosion between Central and Western Sahel. *Aeolian Research*, 2023, 62, pp.100879. 10.1016/j.aeolia.2023.100879 . hal-04278629

HAL Id: hal-04278629

<https://hal.science/hal-04278629v1>

Submitted on 10 Nov 2023

HAL is a multi-disciplinary open access archive for the deposit and dissemination of scientific research documents, whether they are published or not. The documents may come from teaching and research institutions in France or abroad, or from public or private research centers.

L'archive ouverte pluridisciplinaire **HAL**, est destinée au dépôt et à la diffusion de documents scientifiques de niveau recherche, publiés ou non, émanant des établissements d'enseignement et de recherche français ou étrangers, des laboratoires publics ou privés.

A contrasting seasonality of wind erosivity and wind erosion between Central and Western Sahel

Pierre C.^{1}, Rajot JL.^{1,2}, Faye I.³, Dorego G. S.³, Bouet C.^{1,2}, Marticorena B.⁴, Bergametti G.², Ka A.³, Amar B.³, Tall A.³, Diagne N.³, Feron A.²*

¹ *Institute of Ecology and Environmental Sciences (iEES-Paris), Paris, France*

² *Université Paris Cité and Univ Paris Est Creteil, CNRS, LISA, F-75013 Paris, France*

³ *Centre National de la Recherche Agronomique (CNRA), Bambey, Senegal*

⁴ *Univ Paris Est Creteil and Université Paris Cité, CNRS, LISA, F-94010 Créteil, France*

**caroline.pierre@sorbonne-universite.fr*

4 place Jussieu, 75005 Paris, France

Abstract

Wind erosion is a major phenomenon in the Sahel, and can affect soil fertility. Studies of Sahelian aeolian erosion or erosivity are scarce and have been mainly focused on the Central Sahel. Since February 2020, the number of saltating particles and the horizontal flux of aeolian sediment were monitored in Bambey (Senegal) in combination with long-term 5-minutes wind measurements (2014-2021). These datasets enabled to assess the consistency of wind erosion and wind erosivity estimates, and thus to further analyze wind erosivity over pluriannual periods, as wind speed time-series are available over longer terms than horizontal aeolian flux. As a result, the seasonality of wind erosivity largely differs between Western and Central Sahel. In Western Sahel, wind erosivity is related to medium wind speeds during the dry season, while in Central Sahel it is mostly due to high wind speeds occurring at the monsoon onset. Additionally, horizontal flux of aeolian sediments during the dry season are of the same order in Senegal as in Western Niger, but lower than in Eastern Niger. Horizontal flux of aeolian sediments during the rainy season are lower in Senegal than in Western Niger and Eastern Niger. Altogether, annual aeolian flux thus appears significantly lower in Western than in Central Sahel, and mostly related to the dry season.

Keywords: aeolian flux, dust uplift potential, dust emissions, West Africa, dry season, rainy season

1 1. Introduction

2 Wind erosion induces the injection of massive amounts of soil particles into the atmosphere, of about
3 1000 to 4000 Tg per year (*Boucher et al., 2013*). It affects the atmospheric radiative budget (e.g. *Miller*
4 *et al., 2014*), rainfall or ice nucleation (e.g. *Sassen et al., 2003*), and soil fertility through loss and
5 deposition of soil nutrients (*Li et al., 2008; Sterk, 2003*). It has also impacts on human health (e.g. *Goudie,*
6 *2014*) and transports (*Middleton, 2017; Tong et al., 2023*). These issues are of paramount importance
7 in the Sahel, where demographic growth and climate change are large (e.g. *Dosjo and Panitz, 2016;*
8 *Garenne, 2016; Monerie et al., 2020*).

9 Wind erosion occurs when wind speed exceeds a threshold that depends on surface characteristics
10 (namely, obstacles to the wind drag, like vegetation cover, and soil moisture, that increases the cohesion
11 between soil grains). Existing studies based on ground observations show that in the Sahelian region of
12 Mali and Niger, the seasonality of high wind speeds is related to Mesoscale Convective Systems (MCS)
13 and to the Nocturnal Low Level Jet (NLLJ) (e.g. *Bergametti et al., 2017; Marsham et al., 2011*). MCS are
14 convective systems typically of about 100 km large (*Houze, 2004*) occurring during the Sahelian rainy
15 season that induce the highest annual wind speeds but over short time periods (typically less than 30
16 minutes before the rain starts and prevents wind erosion) (*Bergametti et al., 2016; 2022*). NLLJ is a daily
17 meteorological phenomenon due to air stratification during the night; in the morning, the heating of
18 the soil surface induces thermal turbulence of air masses, and thus surface wind speeds that can exceed
19 the threshold wind velocity (e.g. *Fiedler et al., 2013; Knippertz and Todd, 2012; Lothon et al. 2008*).
20 These large wind speeds are mostly westerlies during the rainy season (May to October) and easterlies
21 during the rest of the year (*Lothon et al. 2008; Kaly et al., 2015*).

22 Wind erosion in Central Sahel is maximum in spring (e.g. *Abdourhamane Toure et al., 2011*). This period
23 corresponds to the largest occurrence of high wind speeds and to the lowest vegetation coverage, that
24 roughly coincide in these areas (*Bergametti et al., 2020*). Yet, MCS and NLLJ relative contributions to
25 annual wind erosivity (i.e., the potential of wind to erode) differ between Western and Eastern Niger,
26 with a larger proportion due to the dry-season (monsoonal) wind regime in Eastern (Western) Niger,
27 suggesting that dry-season surface wind speed could decrease from Eastern to Western Niger
28 (*Abdourhamane Touré et al., 2019*).

29 Such detailed analysis has not been performed yet for Western Sahel. However, it is necessary to
30 characterize the seasonality of wind erosivity in this area, in order to improve the understanding of this
31 phenomenon both at the scale of the Sahel, for its remote impacts on climate and nutrients transfer,
32 and at the local scale, for its link to agro-pastoral practices that might mitigate it (*Pierre et al., 2018*).
33 Some studies suggest a distinct seasonality in this area compared to Central Sahel. For example, *Youm*
34 *et al. (2005)* identified maximum wind speed in March over 1998-1999 for 5 sites located on the

35 Senegalese coast. Accordingly, several authors noticed wind erosion, reduced visibility or dust storms in
36 Senegal during the dry season, mostly from January to March (*Aubert et al.*, 1947; *N'tchayi Mbourou et*
37 *al.*, 1997; *Leon et al.*, 2009). Accordingly, *Marticorena et al.* (2017) reported a low contribution of wet
38 dust deposition to total dust deposition in Senegal (Mbour) compared to Mali (Cinzana) and Niger
39 (Banizoumbou) over 2006-2011, suggesting that dry season provides the largest contribution to total
40 dust deposition in Western Sahel.

41 Further analysis is needed to specify the contribution of dry and rainy seasons to wind erosivity and
42 wind erosion in Western Sahel on a pluriannual time-scale. We analyze long-term (2014-2021) 5-
43 minutes wind measurements from a meteorological station of the International Network to study
44 Deposition and Atmospheric chemistry in Africa (INDAAF) in Bambey (Senegal), and 1-year (2020) joint
45 observations of wind speed and wind erosion flux set up from a project dedicated to wind erosion over
46 a groundnut cropland in Sahelian Senegal (ENCAS project) located on the same site. The results are
47 compared to similar observations from other study sites across the Sahel to highlight their respective
48 seasonality.

49 **2. Material and Methods**

50 **2.1. Approach**

51 The monitoring of horizontal sediment flux with a good temporal resolution (e.g. every 1 or 2 weeks)
52 requires frequent field work. This limitation in terms of feasibility, especially in the Sahelian area, implies
53 that pluriannual datasets of horizontal flux of aeolian sediments are rarer than meteorological data like
54 wind speed time-series. Therefore, this study will notably focus on the assessment of wind erosivity over
55 pluriannual periods, following an approach now largely used in the literature (e.g. *Marsham et al.*, 2011;
56 *Cowie et al.*, 2013, 2014, 2015; *Largerou et al.*, 2015; *Bergametti et al.*, 2017, 2022).

57 To thoroughly support this approach, we use 1-year joint measurements of three independent variables
58 (wind speed, horizontal flux of aeolian sediments, and Saltiphone counts) to infer the wind speed
59 threshold required to estimate wind erosivity of the longer-term wind speed time-series. A critical step
60 to ensure the reliability of this approach will be the comparison of the so obtained wind erosivity with
61 horizontal flux of aeolian sediments and Saltiphone counts over their common period of measurement.

62 In addition, to extend the analysis to the whole Sahelian area, results from Senegal will be compared to
63 results from Niger (Banizoumbou, 13.54° N, 2.66° E) and Mali (Cinzana, 13.28°N, 5.93° W) (*Marticorena*
64 *et al.*, 2010).

65

66 **2.2 Site and measurements**

67 Bambeý site is located in the Groundnut Basin (14.43°N; 16.29°W), on lands of the agronomical research
68 station (Centre National de Recherche Agronomique - CNRA) of the Senegalese Institute for Agronomic
69 Research (Institut S n galais de Recherches Agronomiques - ISRA), about 60 km from the coast and 100
70 km east of Dakar (*Figure 1*). It is part of the Western Sahel as defined by several authors (e.g. *Lebel and*
71 *Ali, 2009; Cowie et al., 2015*). The current annual rainfall is approximately 500 mm. Soils are mostly
72 sandy, with sand content of about 90% or more (e.g. *Faye et al., 2018*).

73 Since 2013, a dust monitoring station from the INDAAF network has been deployed. Here, we use
74 INDAAF 5-minute wind speed and wind direction measured at 6.0 m above ground level (agl) using a 2
75 dimensional (2D) sonic anemometer (WindSonic™ Gill Instruments Ltd), and 5-minute rainfall measured
76 at 1.07 m agl with an ARG100 Tipping Bucket rain gauge (Campbell® Scientific company). The accuracy
77 of these instruments is +2% at 12 m.s⁻¹, +3°, and +1% at 20 mm.h⁻¹ and their detection threshold is
78 0.01 m.s⁻¹, 1°, and 0.2 mm, respectively. Over the study period (2014-2021), INDAAF missing wind data
79 were less than 5% in all years but 2017, which thus was discarded for the analysis.

80 In order to measure horizontal flux of aeolian sediment, wind erosion threshold, and aerodynamic
81 roughness length, instruments were set up in February 2020 in the framework of the ENCAS (Erosion
82  olienNe en zone de Culture d'Arachide au Sahel) research project (*Figure 1*). In a groundnut field of
83 about 100 m x 100 m (1 km from the INDAAF station), we installed a rain gauge and 5 anemometers
84 (same as INDAAF) at 0.25m, 0.66m, 1m, 1.5m, and 1.9m agl, and a Saltiphone (*Van Pelt et al., 2009*) at
85 0.08 m agl, that detects the impacts of saltating grains. These measurements were performed with 5-
86 minute time resolution. Missing data were less than 1% over 2020 for these ENCAS dataset (wind speed
87 and Saltiphone). Simultaneously, horizontal sediment flux was monitored using five masts of 5 sand
88 traps each (Modified Wilson and Cooke – MWAC; *Kuntze et al., 1990; Goossens et al., 2000*) at heights
89 of 0.05m, 0.1m, 0.2m, 0.4m, 0.8m agl, set up downwind the main wind directions of the study plot, i.e.
90 at its southwestern corner. They were collected approximately every 2 weeks and their content was
91 weighed with 1 mg precision. Variability of the horizontal sediment flux measured with these devices is
92 discussed in section 2.2. The groundnut field was made bare and tilled during February 2020; wind speed
93 (sand traps) measurements started on February 22nd (24th). Then, groundnut was cropped during the
94 rainy season (short-cycle cultivar, sown on July 8th and 20th because of labor availability, and harvested
95 on October 26th).



96
 97 *Figure 1: Up right: Location of Bambeý study site in Senegal; Bottom left: drone image of the ENCAS*
 98 *study-site. Instruments were set-up at its southwestern corner (red star). Bottom right: Picture of the*
 99 *ENCAS instruments.*

100

101 **2.3 Horizontal flux computation**

102 For each sampling period, the horizontal flux density $q(z)$ ($\text{kg}\cdot\text{m}^{-2}$) was obtained by dividing the mass of
 103 windblown sediments caught in MWAC samplers by their inlet area ($0.50 \cdot 10^{-4} \text{ m}^2$). The horizontal flux
 104 densities were then integrated for each mast to compute the horizontal mass flux ($\text{kg}\cdot\text{m}^{-1}$) between 0
 105 and 0.8 m agl by fitting an exponential equation (least squares method) as proposed by *Fryrear and*
 106 *Saleh (1993)*:

$$107 \quad q(z) = a e^{(-bz)} \quad (1)$$

108 where a and b are adjustment coefficients with units of $\text{kg}\cdot\text{m}^{-2}$ and m^{-1} respectively. The mean of
 109 horizontal flux is then computed from the 5 MWAC masts. Mean coefficient of variation among the 5
 110 masts was low (44%), and even lower (24%) for the main erosive period.

111

112 **2.4 Dust Uplift Potential**

113 The potential erosivity of wind can be assessed by the Dust Uplift Potential (DUP), as defined by
 114 *Marsham et al. (2011)*:

$$115 \quad DUP(z) = u(z)^3 \left(1 + \frac{u_t(z)}{u(z)}\right) \left(1 - \frac{u_t(z)^2}{u(z)^2}\right) \quad \text{for } u > u_t, \text{ and } 0 \text{ otherwise} \quad (2)$$

116 where $u(z)$ is the wind speed at height z and $u_t(z)$ is the threshold wind speed for wind erosion.

117

118 The DUP provides information on the ability of wind to induce wind erosion (wind erosivity), which
119 occurs above the threshold wind speed u_t (see 2.5). The DUP is computed (from the 5-minute wind
120 measurements) for the whole year with a constant threshold corresponding to a bare surface to depict
121 the maximum potential of wind to erode.

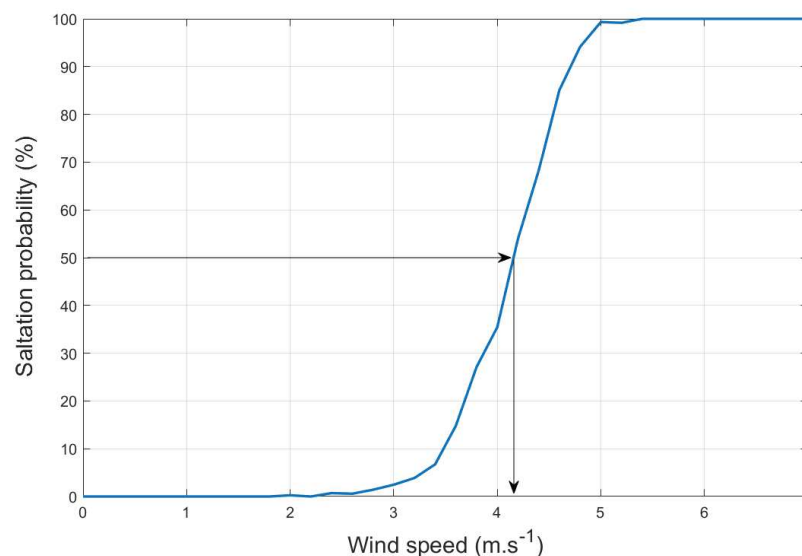
122 An inhibition effect related to rainfall can be accounted for when computing the DUP, as a proxy of the
123 soil moisture effect. Here, rainfall inhibition on DUP is estimated (in 3.1 only) by setting DUP to 0 if
124 $\text{rain} > 0.4$ mm in 1 hour, during the rain and 12 hours after its end, following Bergametti et al. (2017).

125

126 2.5 Salthphone and wind erosion threshold

127 We used the methodology proposed by Abdourhamane Toure et al. (2011) to assess the threshold wind
128 speed u_t required to compute the DUP. As u_t stands for a dry and bare surface (see 2.4), we selected
129 measurements from March 1st, 2020 to May 31st, 2020 that corresponds to a bare soil, before the onset
130 of rainfall season and vegetation growth. Following Abdourhamane Toure et al. (2011), we used
131 Salthphone and wind measurements acquired on the ENCAS-plot and estimated u_t from the probability
132 of saltation occurrence depending on wind speed class. Like these authors, we used wind speed classes
133 of $0.2 \text{ m}\cdot\text{s}^{-1}$ (from 0 to $15 \text{ m}\cdot\text{s}^{-1}$). For each wind speed class, the probability of saltation is the ratio of the
134 number of 5-minute periods during which Salthphone counts were recorded, divided by the total
135 number of 5-minute periods. For each month, the wind erosion threshold is defined as the class of wind
136 speed with the probability of saltation occurrence of 50% (Figure 2). We get $u_{t \text{ ENCAS}}(1.9 \text{ m}) = 4.14 \text{ m}\cdot\text{s}^{-1}$
137 $(\pm 0.07 \text{ m}\cdot\text{s}^{-1})$ as the mean of the three monthly threshold values over this period.

138

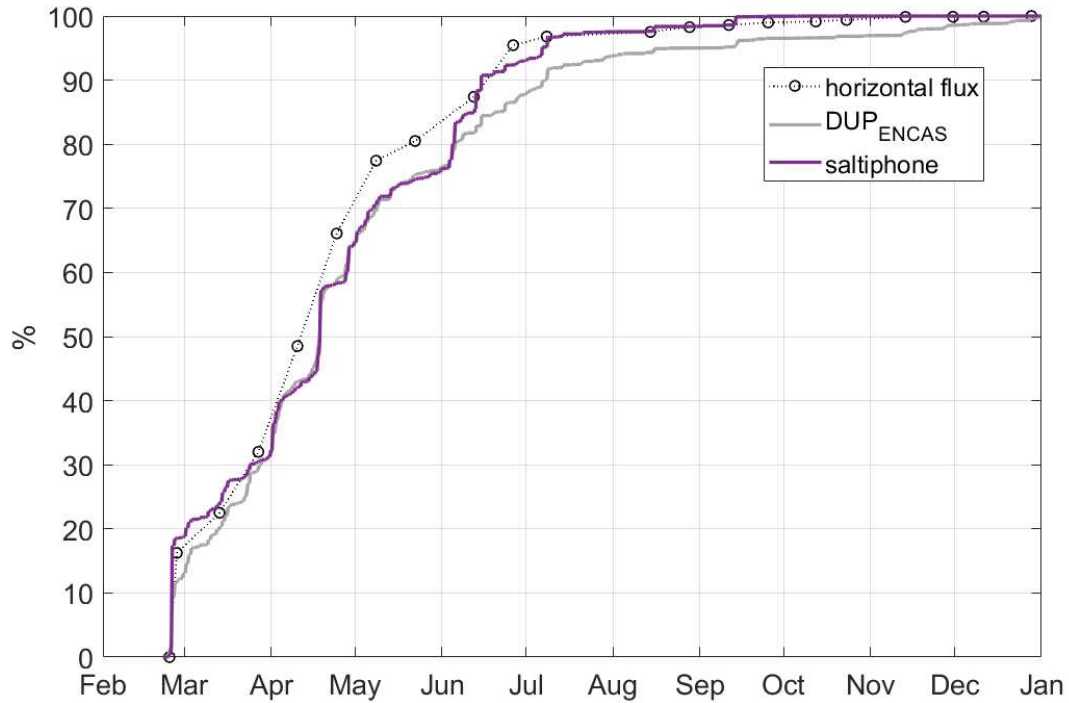


139

140 Figure 2: Wind erosion threshold $u_{t \text{ ENCAS}}(1.9 \text{ m})$ estimation for March 2020

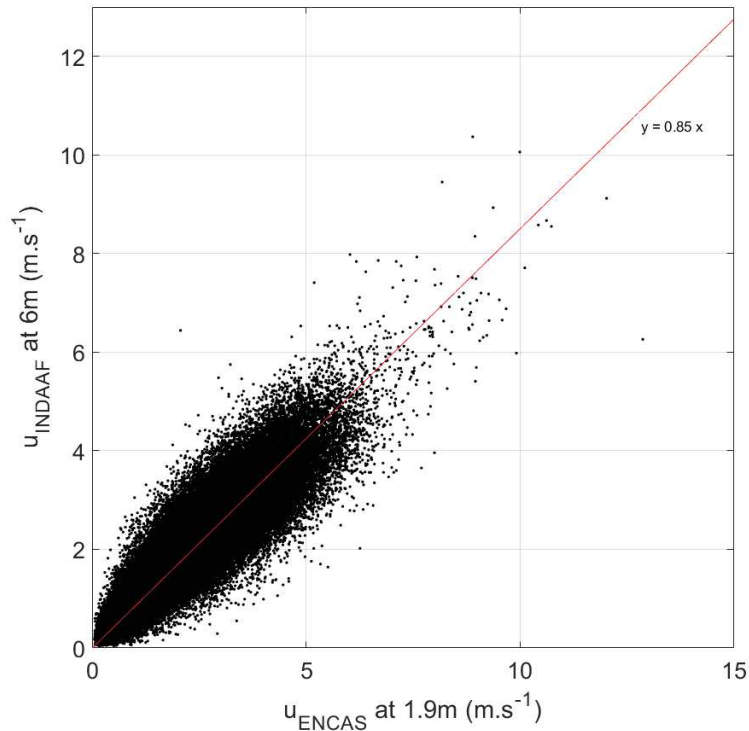
141

142 Using this threshold value, DUP_{ENCAS} exhibits a remarkable agreement with both Saltpphone number
 143 of counts and horizontal flux of aeolian sediments (Figure 3). These three datasets being independent,
 144 this ensures the reliability of the threshold value.
 145



146
 147 *Figure 3: Normalized cumulative annual horizontal flux of aeolian sediments, DUP_{ENCAS} , and*
 148 *Saltpphone counts in Bambej over March-December 2020 ($R=0.99$ and $n=21$ between horizontal flux*
 149 *and Saltpphone counts, and between horizontal flux and DUP_{ENCAS}).*

150
 151 The wind erosion threshold was then applied to u_{INDAAF} to assess the DUP over the whole time-period
 152 of INDAAF measurements. The correlation coefficient between measured wind speeds $u_{INDAAF}(6\text{ m})$
 153 and $u_{ENCAS}(1.9\text{ m})$ (the highest ENCAS anemometer) over February 22nd – December 31st, 2020 is $R=$
 154 0.92 ($n=89461$) with a proportional coefficient of 0.85 (Figure 4). $u_{INDAAF}(6\text{ m})$ is lower than
 155 $u_{ENCAS}(1.9\text{ m})$ as it is located in a slight lowland and surrounded by scattered woody vegetation, but
 156 exhibits the same dynamics. The translation of u_{INDAAF} to the ENCAS-plot (to compute the DUP using
 157 the same threshold of $4.14\text{ m}\cdot\text{s}^{-1}$) was thus performed using this proportional coefficient of 0.85
 158 between $u_{ENCAS}(1.9\text{ m})$ and $u_{INDAAF}(6\text{ m})$.
 159



160

161 *Figure 4: Scatterplot of wind speed at INDAAF station (at 6m) versus at ENCAS study site (at 1.9m) on*
 162 *the period February 22nd to December 31st, 2020 (R=0.92; n=89461)*

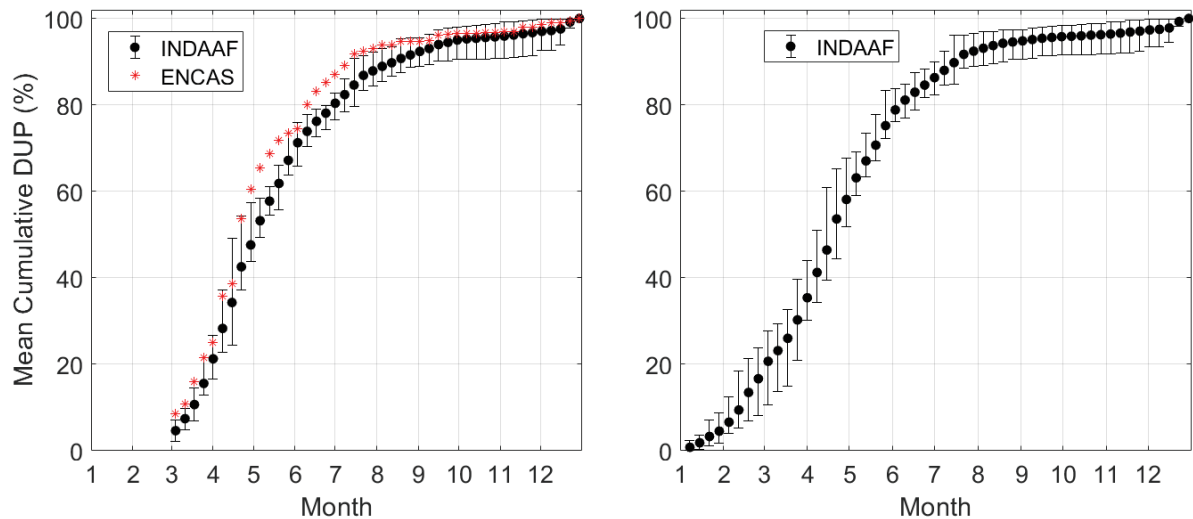
163

164 3. Results and Discussion

165 3.1 Dust Uplift Potential

166 In order to further assess the reliability of the threshold wind speed applied to u_{INDAAF} , DUP_{INDAAF}
 167 was computed over 2014-2021 over March-December (to be compared to DUP_{ENCAS} over March-
 168 December 2020) and over the whole year (*Figure 5*). Normalized cumulated DUP_{ENCAS} shows a clear
 169 seasonality with about 40% of the 10-month DUP accumulated between the beginning of March and
 170 mid-April, and almost no erosive wind from mid-July to mid-December, similarly to the pluriannual mean
 171 of normalized cumulated DUP_{INDAAF} . Over the whole year, DUP_{INDAAF} reaches 20% of the annual DUP
 172 at the beginning of March, 50% around mid-April, and about 90% mid-July. In addition, DUP_{INDAAF}
 173 shows a clear climatological signal as it exhibits a very low interannual variability (minimum and
 174 maximum weekly values of the normalized cumulated DUP, reported in *Figure 5*, usually differ from the
 175 average value by about 5%, sometimes up to 10%). Thus, this 7-year mean DUP obtained for the
 176 Senegalese study site can be compared to 9-year mean DUP analyzed in previous work for two study
 177 sites in Central Sahel (*Bergametti et al., 2017*), that also show a clear climatological signal over 9-year
 178 time-series (see Fig. 5 in *Bergametti et al., 2017*).

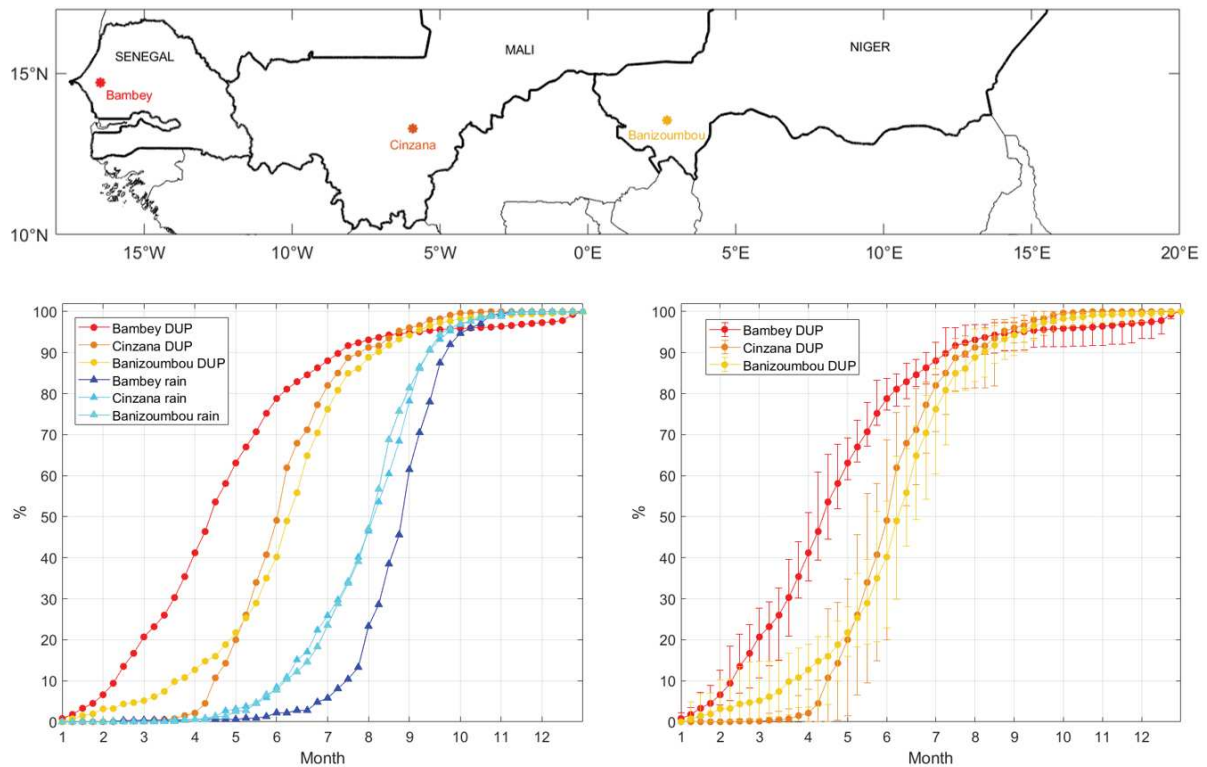
179



180
 181 *Figure 5: Annual cumulative DUP in Bambeý averaged at a weekly time-step. Minimum and maximum*
 182 *over the period (vertical bars) are also reported for INDAAF data. Left: Cumulated and normalized over*
 183 *March-December 2014–2021 (but 2017) for INDAAF, 2020 for ENCAS. Right: Same as left panel but*
 184 *over the whole year, for INDAAF data only.*

185
 186 This comparison shows that the seasonality of wind erosivity in Senegal (Bambeý) is different from
 187 Southwestern Niger (Banizoumbou) and Central Mali (Cinzana) over 2006-2015 (*Figure 6*), where the
 188 proportion of annual DUP sharply increases from 20% to 50% between early May and early June. *Figure*
 189 *6* also shows that the 3 month-period producing the largest proportion (more than 50 %) of annual DUP
 190 in Bambeý is February-March-April, whereas it is April-May-June in Banizoumbou and Cinzana
 191 (respectively about 60% and 80%). However, about 90% of the annual DUP is reached in early August
 192 for the three sites. Additionally, although there is a non-negligible range between minimum and
 193 maximum weekly values of DUP, the seasonality of wind erosivity in Bambeý is clearly distinct from the
 194 ones of Cinzana and Banizoumbou.

195 The comparison of the seasonality of normalized cumulated DUP and normalized cumulated rainfall
 196 further shows that the first significant rains occur in Bambeý by the beginning of June, reaching about
 197 10% of the annual rainfall around mid-July. In Cinzana and Banizoumbou, they occur by the beginning
 198 of May and 10% of the annual rainfall is reached around early June, i.e. about one month earlier than in
 199 Bambeý. *Kaly et al. (2015)* also observed, in Mbour (on the Senegalese coast, 80 km south of Dakar), no
 200 increase in the monthly mean wind speed during the rainy season but a maximum in February-March
 201 and a later onset of the rainy season than for Cinzana and Banizoumbou. In the following, rainy-season
 202 is thus defined as May-October in Bambeý, and April-October in Banizoumbou and Cinzana (as in
 203 *Bergametti et al., 2017*), with the dry season encompassing the rest of the year.

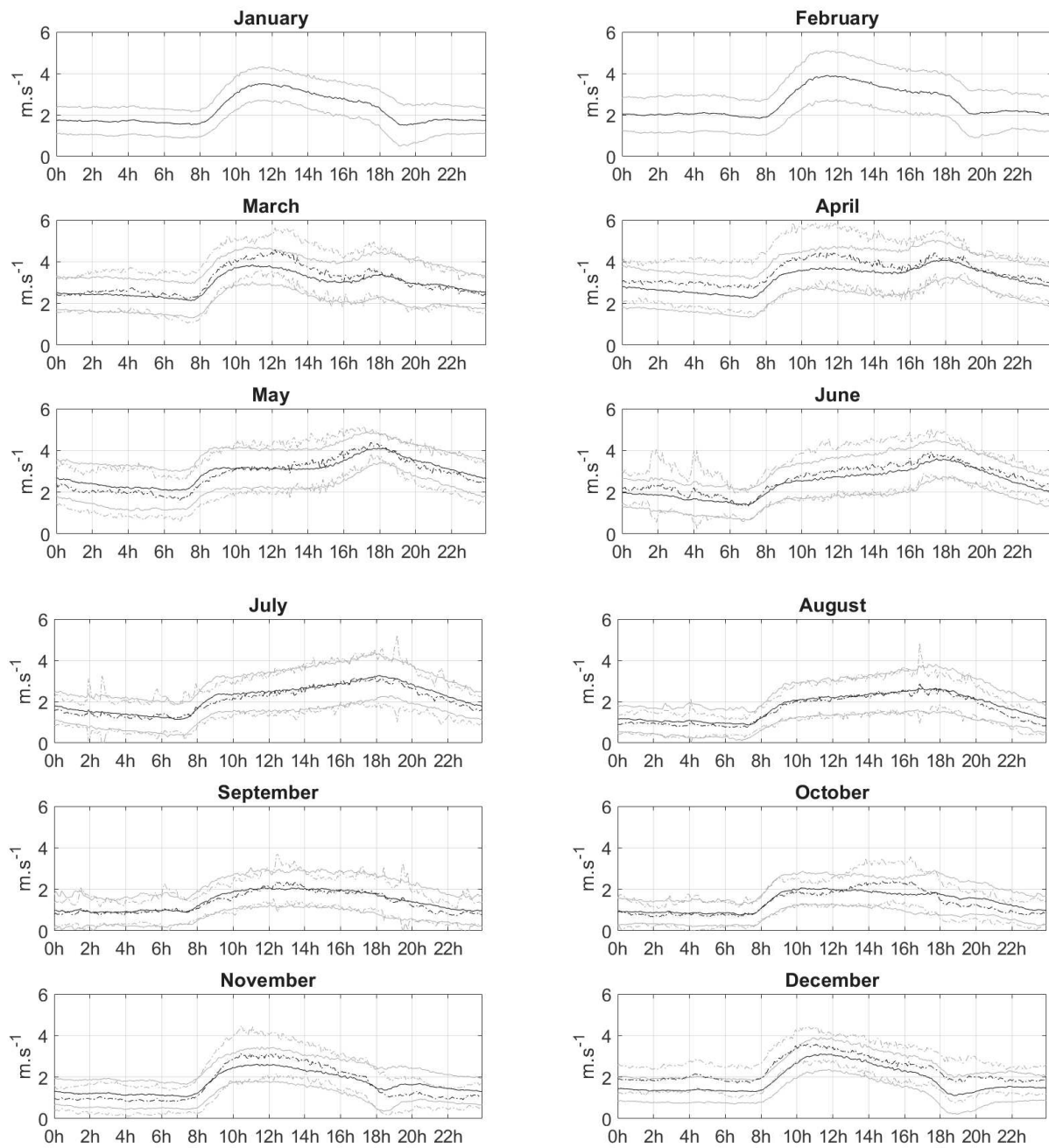


205
 206 *Figure 6: Top: Location of the three Sahelian sites; Bottom left: Annual cumulative DUP and rainfall*
 207 *averaged over 2014–2021 (but 2017) in Bambeý (Senegal), 2006–2015 (but 2007) in Cinzana (Mali)*
 208 *and 2006–2015 (but 2014) in Banizoumbou (Niger), at a weekly time-step. Bottom right: idem for DUP*
 209 *only, with minimum and maximum over each weekly period (vertical bars). Figure adapted from Fig. 7*
 210 *in Bergametti et al. (2017)*

211
 212 In Bambeý, about 60% of wind erosivity is thus related to the dry season, but only 2% in Cinzana and
 213 14% in Banizoumbou. In Bambeý, the DUP shows a non-negligible contribution of December (22% of
 214 annual DUP in 2016 and 2021, and between 0 and 5% for the other years; not shown) whereas this
 215 contribution is much lower in Banizoumbou (0.6% in average) and nil in Cinzana. Altogether, DUP
 216 inhibition related to rain in Bambeý is thus very low, ranging from 2% (in 2016) to 6% (in 2014) of annual
 217 DUP, whereas it is about 25% for Banizoumbou and Cinzana (Bergametti et al., 2017).

218 Our observations are in agreement with the characteristics of MCS observed in the Sahelian area. These
 219 MCS usually form in Eastern and Central Sahel and propagate westward (Houze, 2004; Futyán and Del
 220 Genio, 2007), reaching their maximum intensity before weakening when approaching Western Sahel
 221 (Roca et al., 2005; DeLonge et al., 2010), with typical trajectory from genesis to lysis of about 1000 km
 222 and a typical lifetime of about 1 day (Vizy and Cook, 2018). Wind erosivity in western Sahel is thus mostly
 223 due to the winds occurring during the dry season.

224



225

226

227 *Figure 7: Diurnal cycle of wind speed: 2014-2021 pluriannual mean of the 5-minutes INDAAF values*
 228 *averaged over each month and their standard deviation (continuous lines); idem for ENCAS wind speed*
 229 *but on the period March 1st to December 31st, 2020 (dotted lines)*

230

231 In order to check if high wind speeds in Bambey were related to NLLJ, we analyzed the diurnal cycle of
 232 wind speed (*Figure 7*): it exhibits a slight increase in the morning during the dry season, likely related to
 233 the NLLJ, yet in a lesser extent than for the other Sahelian sites (see Fig. 1 in *Bergametti et al., 2022*). It

234 also exhibits a daily maximum in the late afternoon during the end of the dry season and the rainy
 235 season, which differs from other Sahelian study sites.
 236

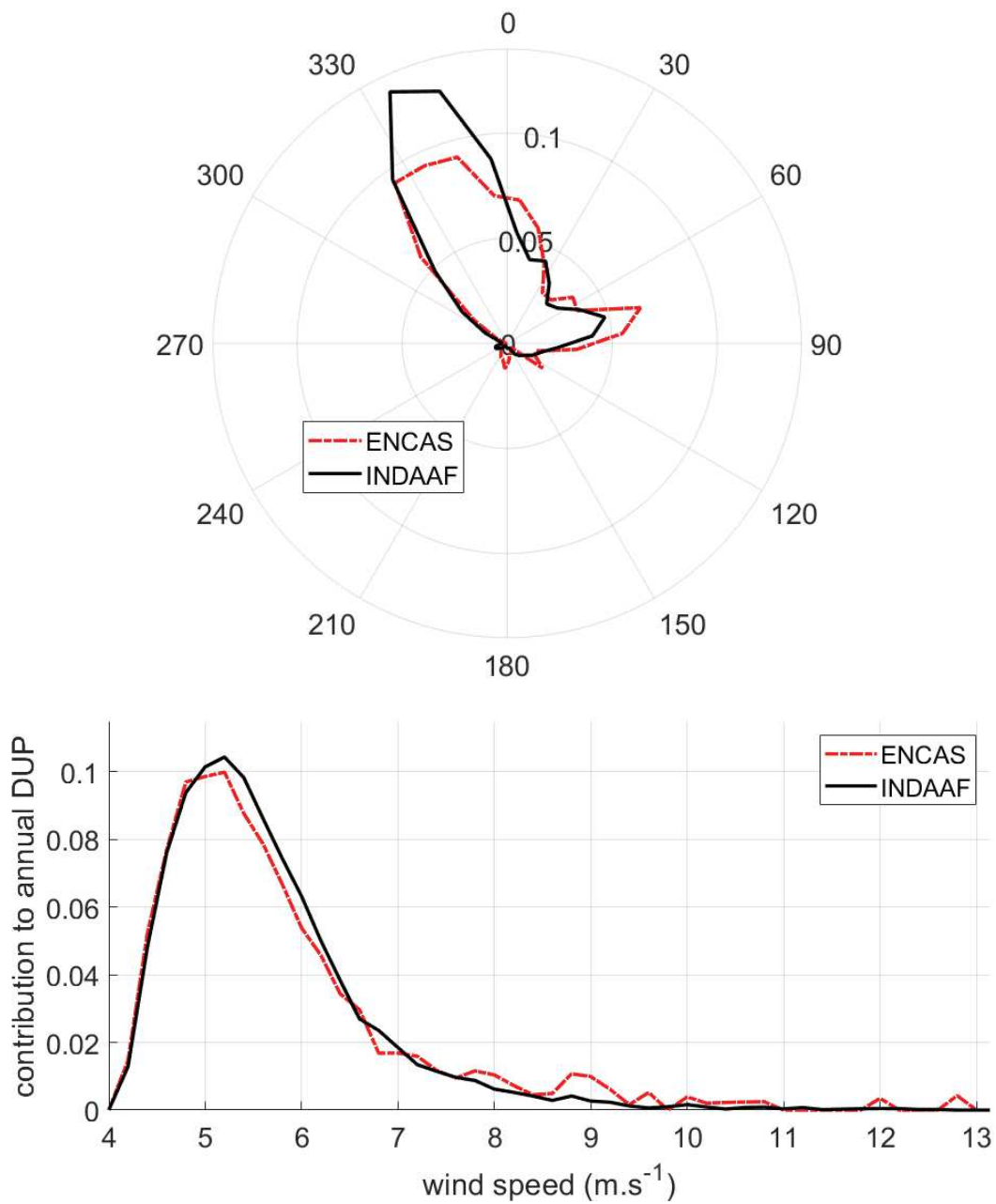


Figure 8a: Contribution to annual DUP by wind direction in Bambeý: INDAAF 2014-2021 pluriannual mean (black); ENCAS March 1st to December 31st, 2020 (red).

8b: Contribution to annual DUP by wind speed over 2014–2021 (but 2017) in Bambeý: INDAAF 2014-2021 pluriannual mean (black); ENCAS March 1st to December 31st, 2020 (red)

237

238 A large proportion of annual DUP in Bambeý is provided by north-northwestern winds, as illustrated for
 239 both ENCAS and INDAAF wind measurements in Figure 8a. In terms of pluriannual mean (INDAAF

240 measurements), 35% of annual DUP is provided by directions 320°- 350° (potentially related to the sea
 241 breeze), thus as much as the proportion of DUP (35%) provided by northern to eastern winds (0°-90°,
 242 i.e. Harmattan wind regime). The contribution of winds blowing from other directions (90°-320°) is low
 243 (21%); more specifically, contribution of winds from 150°-300° is about 5% of the annual DUP.
 244 Accordingly, *Kaly et al.* (2015) observed in Mbour almost no southwestern winds.
 245 Furthermore, a large part of annual DUP in Bambey is due to wind speeds ranging between 4.14 and 6
 246 m.s⁻¹, for both ENCAS and INDAAF measurements (*Figure 8b*). In terms of pluriannual mean (INDAAF
 247 measurements), 76% of annual DUP is provided by these wind speed classes, and 16% by wind speeds
 248 ranging between 6 and 7 m.s⁻¹. Only 3% of the annual DUP is related to wind speeds larger than 8 m.s⁻¹
 249 ¹, and 1% to wind speed larger than 10 m.s⁻¹. This is in agreement with results by *Cowie et al* (2015) who
 250 observed a narrow shape of wind speeds contribution to DUP just above the threshold for western
 251 Sahel.

252

253 3.2 Aeolian flux

254 The analysis of the seasonality of wind erosivity across the Sahel can be further substantiated by
 255 scrutinizing the few recent measurements of local wind erosion in this area. The horizontal flux of
 256 aeolian sediments (G) in Bambey (2020) exhibits a marked seasonality (*Figure 3*), with about 70% of the
 257 annual flux accumulating from late February (start of measurements) to the end of April. This seasonality
 258 is in agreement with that observed by *Niang* (2019) in northern Senegal. G measured in Bambey
 259 amounted 564 kg.m⁻¹ from February 24th to December 31st, 2020.

260 As the ENCAS-plot was made bare at the beginning of ENCAS monitoring, and as wind erosivity for this
 261 study site is very low during the rainy season (i.e. when vegetation starts growing), the most relevant
 262 comparison to existing measurements in the Sahel is with other bare surfaces (*Table 1*). Over the dry
 263 season only, G in Bambey (Senegal) reaches comparable amounts as for a bare surface in Banizoumbou
 264 (Western Niger) over 2006-2008. As the rainy-season contribution to annual G is very low in Bambey
 265 compared to Banizoumbou, annual G is also much lower. Dry-season and rainy-season G in Bambey are
 266 both much lower than observations for a bare dune in Kilakina (southeastern Niger, 13.72°N, 10.75°E)
 267 over 2012-2016. Annual flux is thus much larger in Kilakina than in Bambey.

268

	Bambey 2020	Banizoumbou (2006-2008)	Kilakina (2012-2016)
<i>G dry season (kg.m⁻¹)</i>	405	388 +/- 96	2047 +/- 1207
<i>G rainy season (kg.m⁻¹)</i>	159	828 +/- 490	2180 +/- 1014
<i>G total (kg.m⁻¹)</i>	564	1461 +/- 446	4228 +/- 1669
<i>Prop dry season (%)</i>	72	27 +/- 1	44 +/- 23

<i>Prop rainy season (%)</i>	28	73 +/- 1	56 +/- 23
------------------------------	----	----------	-----------

269 *Table 1: Horizontal flux amounts (kg.m⁻¹) and proportion for the rainy season and dry-season in*
270 *Bambey (Senegal; this study), Banizoumbou (western Niger; Abdourhamane Toure et al., 2011), and*
271 *Kilakina (eastern Niger; Abdourhamane Touré et al., 2019), for a bare surface.*

272
273 Altogether, this suggests that: (i) wind erosivity during the dry-season would be of similar amplitude in
274 Senegal and Western Niger, but larger in Eastern Niger, and that (ii) the rainy-season wind erosivity is
275 much lower in Western Sahel than in Central Sahel. However, interannual variability of these observed
276 horizontal fluxes is relatively large and these results thus need to be further substantiated by long-term
277 measurements.

278

279 4. Conclusion

280 The combination of datasets from long-term wind measurements (INDAAF) and 10-month wind and
281 wind erosion measurements (ENCAS) provides a deep insight into the seasonal characteristics of wind
282 erosion and wind erosivity in Senegal. The analysis of both datasets demonstrated that the largest
283 proportion of annual wind erosivity in Western Sahel occurs from February to April – thus during the
284 dry-season - and is related to wind speed just above the erosion threshold likely related to a Low Level
285 Jet. This observation clearly differs from what have been observed in Central Sahel, where most wind
286 erosivity is due to high winds from convective systems at the onset of the rainy season (around June).
287 However, amounts of horizontal flux of aeolian sediments during the dry season are of the same order
288 in Senegal and in western Niger, but lower than in eastern Niger. As the rainy season only induces a very
289 low horizontal flux in Senegal, its annual aeolian flux (in mass) is thus sensibly lower than for study sites
290 in Central Sahel.

291 Altogether, our results show that the seasonality of wind erosivity is not homogeneous over the Sahel.
292 MCS are likely to provide less high wind speeds in Senegal than in Central Sahel. Dry-season wind
293 erosivity in Western Sahel is similar to that in Western Niger, which is lower than in Eastern Niger. Rainy-
294 season wind erosivity decreases from Western Niger to Senegal, but with approximately similar
295 amplitude between Eastern and Western Niger. Thus, in order to prevent wind erosion and soil nutrients
296 depletion (e.g. through land use practices), attention should be paid to the location in the Sahel and the
297 associated seasonality of erosive winds. Further investigations are needed to interpret this contrasted
298 seasonality in relation with climate mechanisms in the Sahel.

299

300 Acknowledgements

301 The French National Observatory Service INDAAF is supported by the INSU/CNRS, the IRD (Institut de
302 Recherche pour le Développement), and the Observatoire des Sciences de l'Univers EFLUVE and
303 Observatoire Midi-Pyrénées. This work was supported by the ENCAS (Erosion éolienne d'une surface
304 Cultivée en Arachide au Sahel) research program funded by LEFE-EC2CO fund call of the French National
305 Institute of Sciences of the Universe (INSU). The authors would like to thank the French and African PIs
306 and operators for maintaining the INDAAF and ENCAS stations and for the ENCAS monitoring.

307

308 **Data Availability Statement**

309 The INDAAF data are distributed through the INDAAF website (<https://indaaf.obs-mip.fr/catalogue>). The
310 ENCAS data used in this manuscript are available for download for research and educational purposes
311 in DataSuds (<https://doi.org/10.23708/LNZLZF>).

312

313 **Références**

314 Abdourhamane Touré, A., Rajot, J. L., Garba, Z., Marticorena, B., Petit, C., & Sebag, D. (2011). Impact of very low
315 crop residues cover on wind erosion in the Sahel. *Catena*, 85(3), 205–214.
316 <https://doi.org/10.1016/j.catena.2011.01.002>

317

318 Abdourhamane Touré, A. A., Tidjani, A. D., Rajot, J. L., Marticorena, B., Bergametti, G., Bouet, C., ... & Garba, Z.
319 (2019). Dynamics of wind erosion and impact of vegetation cover and land use in the Sahel: A case study on sandy
320 dunes in southeastern Niger. *Catena*, 177, 272-285.

321

322 Aubert, G., Dubois J., Maignien R. (1947). L'érosion éolienne dans le Nord-Ouest du Sénégal : observations
323 effectuées lors de l'exécution d'une mission d'étude des sols à arachide, organisée par l'Office de la Recherche
324 Scientifique Coloniale, et le Service de l'Agriculture de l'Afrique Occidentale Française. In : *Congrès de pédologie
325 méditerranéenne*. sl : AFES, p. 443-450. Conférence de Pédologie Méditerranéenne, Montpellier; Alger (FR; DZ),
326 1947/05/09-20)

327 Bergametti, G., Rajot, J. L., Pierre, C., Bouet, C., & Marticorena, B. (2016). How long does precipitation inhibit wind
328 erosion in the Sahel? *Geophysical Research Letters*, 43, 6643–6649. <https://doi.org/10.1002/2016GL069324>

329

330 Bergametti, G., Marticorena, B., Rajot, J. L., Chatenet, B., Féron, A., Gaimoz, C., ... & Zakou, A. (2017). Dust uplift
331 potential in the Central Sahel: an analysis based on 10 years of meteorological measurements at high temporal
332 resolution. *Journal of Geophysical Research: Atmospheres*, 122(22), 12-433.

333

334 Bergametti, G., Marticorena, B., Rajot, J. L., Siour, G., Féron, A., Gaimoz, C., ... & Zakou, A. (2020). The respective
335 roles of wind speed and green vegetation in controlling Sahelian dust emission during the wet season. *Geophysical*
336 *Research Letters*, 47(22), e2020GL089761.

337

338 Bergametti, G., Rajot, J. L., Marticorena, B., Féron, A., Gaimoz, C., Chatenet, B., ... & Zakou, A. (2022). Rain, wind,
339 and dust connections in the Sahel. *Journal of Geophysical Research: Atmospheres*, 127(3), e2021JD035802.

340

341 Boucher, O., Randall, D., Artaxo, P., Bretherton, C., Feingold, G., Forster, P., et al. (Eds.), (2013). *Climate change*
342 *2013: The physical basis. Contribution of working group I to the fifth assessment report of the intergovernmental*
343 *panel on climate change* (pp. 571–657). Cambridge, UK: Cambridge University Press.
344 <https://doi.org/10.107/CBO9781107415324.016>

345

346 Bouniol, D., Couvreur, F., Kamsu-Tamo, P. H., Leplay, M., Guichard, F., Favot, F., & O'Connor, E. J. (2012). Diurnal
347 and seasonal cycles of cloud occurrences, types, and radiative impact over West Africa. *Journal of Applied*
348 *Meteorology and Climatology*, 51(3), 534–553. <https://doi.org/10.1175/JAMC-D-11-051.1>

349

350 Cowie, S. M., Knippertz, P., & Marsham, J. H. (2013). Are vegetation-related roughness changes the cause of the
351 recent decrease in dust emission from the Sahel?. *Geophysical Research Letters*, 40(9), 1868-1872.

352

353 Cowie, S. M., Knippertz, P., & Marsham, J. H. (2014). A climatology of dust emission events from northern Africa
354 using long-term surface observations. *Atmospheric Chemistry and Physics*, 14(16), 8579-8597.

355

356 Cowie, S. M., Marsham, J. H., & Knippertz, P. (2015). The importance of rare, high-wind events for dust uplift in
357 northern Africa. *Geophysical Research Letters*, 42(19), 8208-8215.

358

359 DeLonge, M. S., Fuentes, J. D., Chan, S., Kucera, P. A., Joseph, E., Gaye, A. T., & Daouda, B. (2010). Attributes of
360 mesoscale convective systems at the land-ocean transition in Senegal during NASA African Monsoon
361 Multidisciplinary Analyses 2006. *Journal of Geophysical Research: Atmospheres*, 115(D10).

362

363 Dosio, A., & Panitz, H. J. (2016). Climate change projections for CORDEX-Africa with COSMO-CLM regional climate
364 model and differences with the driving global climate models. *Climate Dynamics*, 46, 1599–1625.
365 <https://doi.org/10.1007/s00382-015-2664-4>

366

367 Faye, B., Webber, H., Diop, M., Mbaye, M. L., Owusu-Sekyere, J. D., Naab, J. B., & Gaiser, T. (2018). Potential impact
368 of climate change on peanut yield in Senegal, West Africa. *Field Crops Research*, 219, 148-159.

369

370 Fiedler, S., Schepanski, K., Heinold, B., Knippertz, P., & Tegen, I. (2013). Climatology of nocturnal low-level jets over
371 North Africa and implications for modeling mineral dust emission. *Journal of Geophysical Research: Atmospheres*,
372 *118*(12), 6100-6121.

373

374 Fryrear, D. W., & Saleh, A. (1993). Field wind erosion: vertical distribution. *Soil Science*, *155*(4), 294-300.

375

376 Futyan, J. M., & Del Genio, A. D. (2007). Deep convective system evolution over Africa and the tropical Atlantic.
377 *Journal of Climate*, *20*(20), 5041-5060.

378

379 Garenne, M. (2016). La pression de la population dans les pays sahéliens francophones: Analyse des estimations
380 et projections de population 1950–2100 (Ferdi Working Pap. 168, p. 26).

381

382 Goossens, D., Offer, Z., & London, G. (2000). Wind tunnel and field calibration of five aeolian sand traps.
383 *Geomorphology*, *35*(3-4), 233-252. [https://doi.org/10.1016/S0169-555X\(00\)00041-6](https://doi.org/10.1016/S0169-555X(00)00041-6)

384 Goudie, A. S. (2014). Desert dust and human health disorders. *Environment international*, *63*, 101-113.

385

386 Houze Jr, R. A. (2004). Mesoscale convective systems. *Reviews of Geophysics*, *42*(4).

387

388 Kaly, F., Marticorena, B., Chatenet, B., Rajot, J. L., Janicot, S., Niang, A., Yah, H., Thiria, S., Maman, A., Zakou, A.,
389 Coulibaly, M., Koné, I., Traoré, S., Diallo, A., & Ndiaye, T. (2015). Variability of mineral dust concentrations over
390 West Africa monitored by the Sahelian Dust Transect. *Atmospheric Research*, *164*, 226-241.

391

392 Knippertz, P., & Todd, M. C. (2012). Mineral dust aerosols over the Sahara: Meteorological controls on emission
393 and transport and implications for modeling. *Reviews of Geophysics*, *50*, RG1007.
394 <https://doi.org/10.1029/2011RG000362>

395

396 Kuntze, H., Beinhauer, R., Tetzlaff, G. (1990). Quantification of Soil Erosion by Wind: I. Final Report of the BMFT
397 project. Project No. 0339058 A, B, C. Institute of Meteorology and Climatology, University of Hannover.

398

399 Llargeron, Y., Guichard, F., Bouniol, D., Couvreux, F., Kergoat, L., & Marticorena, B. (2015). Can we use surface wind
400 fields from meteorological reanalyses for Sahelian dust emission simulations?. *Geophysical Research Letters*, *42*(7),
401 2490-2499.

402

403 Lebel, T., & Ali, A. (2009). Recent trends in the Central and Western Sahel rainfall regime (1990–2007). *Journal of*
404 *Hydrology*, *375*(1-2), 52-64.

405

406 Léon, J. F., Derimian, Y., Chiapello, I., Tanré, D., Podvin, T., Chatenet, B., ... & Deroo, C. (2009). Aerosol vertical
407 distribution and optical properties over M'Bour (16.96° W; 14.39° N), Senegal from 2006 to 2008. *Atmospheric*
408 *Chemistry and Physics*, 9(23), 9249-9261.

409

410 Li, J., Okin, G. S., Alvarez, L., & Epstein, H. (2008). Effects of wind erosion on the spatial heterogeneity of soil
411 nutrients in two desert grassland communities. *Biogeochemistry*, 88, 73–88. [https://doi.org/10.1007/s10533-008-](https://doi.org/10.1007/s10533-008-9195-6)
412 9195-6

413

414 Lothon, M., Said, F., Lohou, F., & Campistron, B. (2008). Observation of the diurnal cycle in the low troposphere of
415 West Africa. *Monthly Weather Review*, 136(9), 3477–3500. <https://doi.org/10.1175/2008MWR2427.1>

416

417 Marsham, J. H., Knippertz, P., Dixon, N. S., Parker, D. J., & Lister, G. M. S. (2011). The importance of the
418 representation of deep convection for modeled dust-generating winds over West Africa during summer.
419 *Geophysical Research Letters*, 38, L16803. <https://doi.org/10.1029/2011GL048368>

420

421 Marticorena, B., Chatenet, B., Rajot, J. L., Bergametti, G., Deroubaix, A., Vincent, J., ... Zakou, A. (2017). Mineral
422 dust over West and Central Sahel: Seasonal patterns of dry and wet deposition fluxes from a pluriannual sampling
423 (2006-2012). *Journal of Geophysical Research: Atmospheres*, 122, 1338–1364.
424 <https://doi.org/10.1002/2016JD025995>

425

426 Marticorena, B., Chatenet, B., Rajot, J. L., Traoré, S., Coulibaly, M., Diallo, A., ... Zakou, A. (2010). Temporal
427 variability of mineral dust concentrations over West Africa: Analyses of a pluriannual monitoring from the AMMA
428 Sahelian Dust Transect. *Atmospheric Chemistry and Physics*, 10(18), 8899–8915. [https://doi.org/10.5194/acp-10-](https://doi.org/10.5194/acp-10-8899-2010)
429 8899-2010

430

431 Middleton, N. J. (2017). Desert dust hazards: A global review. *Aeolian research*, 24, 53-63.

432

433 Miller, R. L., Knippertz, P., Perez Garcia-Pando, C., Perlwitz, J. P., & Tegen, I. (2014). Impact of dust radiative forcing
434 upon climate. In P. Knippertz, & J. B. Stuut (Eds.), *Mineral dust: A key player in the Earth system* (Chapter 11, pp.
435 327–357). Dordrecht, The Netherlands: Springer. https://doi.org/10.1007/978-94-017-8978-3_13

436

437 Monerie, P. A., Wainwright, C. M., Sidibe, M., & Akinsanola, A. A. (2020). Model uncertainties in climate change
438 impacts on Sahel precipitation in ensembles of CMIP5 and CMIP6 simulations. *Climate Dynamics*, 55, 1385–1401.
439 <https://doi.org/10.1007/s00382-020-05332-0>

440 Niang, S. (2019). Sécheresse climatique et dynamique éolienne sur la côte nord du Sénégal : sensibilité dunaire et
441 estimation des débits massiques dans le Gandiolais. NAAJ. *Revue africaine sur les changements climatiques et les*
442 *énergies renouvelables*, 1(1), 111-135. DOI : 10.46711/naaj.2019.1.1.6

443

444 N'Tchayi, G. M., Bertrand, J., & Nicholson, S. E. (1997). The diurnal and seasonal cycles of wind-borne dust over
445 Africa north of the equator. *Journal of Applied Meteorology*, 36, 868–882.

446

447 Pierre, C., Kergoat, L., Hiernaux, P., Baron, C., Bergametti, G., Rajot, J. L., ... & Marticorena, B. (2018). Impact of
448 agropastoral management on wind erosion in Sahelian croplands. *Land Degradation & Development*, 29(3), 800-
449 811.

450

451 Priestley, C.H.B., 1959. Turbulent Transfer in the Lower Atmosphere. *Univ. Chicago Press*, Chicago, 130 p..

452

453 Roca, R., Lafore, J. P., Piriou, C., & Redelsperger, J. L. (2005). Extratropical dry-air intrusions into the West African
454 monsoon midtroposphere: An important factor for the convective activity over the Sahel. *Journal of the*
455 *Atmospheric Sciences*, 62(2), 390-407.

456

457 Sassen, K., DeMott, P. J., Prospero, J. M., & Poellot, M. R. (2003). Saharan dust storms and indirect aerosol effects
458 on clouds: CRYSTAL-FACE results. *Geophysical Research Letters*, 30(12), 1633.
459 <https://doi.org/10.1029/2003GL017371>

460

461 Sterk, G. (2003). Causes, consequences and control of wind erosion in Sahelian Africa: A review. *Land Degradation*
462 *& Development*, 14(1),98–108. <https://doi.org/10.1002/ldr.526>

463

464 Tidjani, A.D., Biielders, C.L., Ambouta, K.J.-M., 2009. Dynamique saisonnière des paramètres déterminant l'érosion
465 éolienne sur les pâturages dunaires du Niger oriental. *Geo-Eco-Trop*. 33, 39–56.

466

467 Tong, D. Q., Gill, T. E., Sprigg, W. A., Van Pelt, R. S., Baklanov, A. A., Barker, B. M., ... & Vimic, A. V. (2021). Health
468 and safety effects of airborne soil dust in the Americas and beyond. *Reviews of Geophysics*, e2021RG000763.

469

470 Van Pelt, R. S., Peters, P., & Visser, S. (2009). Laboratory wind tunnel testing of three commonly used saltation
471 impact sensors. *Aeolian Research*, 1(1-2), 55-62.

472

473 Vizy, E. K., & Cook, K. H. (2017). Mesoscale convective systems and nocturnal rainfall over the west African Sahel:
474 Role of the inter-tropical front. *Climate Dynamics*. <https://doi.org/10.1007/s00382-017-3628-7>

475

476 Youm, I., Sarr, J., Sall, M., Ndiaye, A., & Kane, M. M. (2005). Analysis of wind data and wind energy potential along
477 the northern coast of Senegal. *Revue des Energies Renouvelables*, 8(2), 95-108.

478